frontiers | Frontiers in Energy Research

TYPE Original Research
PUBLISHED 19 December 2024
DOI 10.3389/fenrg.2024.1443269

First downhole sampling of a natural hydrogen reservoir in Colombia

Cesar Patiño[1], Dariusz Strąpoć[2]*, Oscar Torres[3], Oliver Mullins[4], Ulises Bustos[5], Oscar Bermudez[6], Albeiro López[6], Maria Trujillo[7] and Hans Morales[7]

[1]Ecopetrol, Technical Development Center, Bogota, Colombia, [2]SLB, Well Construction Measurements, Clamart, France, [3]SLB, Well Construction Measurements, Bogota, Colombia, [4]SLB, Well Services, Houston, United States, [5]SLB, Reservoir Performance, Houston, United States, [6]Ecopetrol, Reservoir Engineering, Bogota, Colombia, [7]Ecopetrol, Exploration, Bogota, Colombia

OPEN ACCESS

EDITED BY
Guangfu Liao,
Fujian Agriculture and Forestry University, China

REVIEWED BY
Guixiang Ding,
Fujian Agriculture and Forestry University, China
Bin Yang,
Shihezi University, China

*CORRESPONDENCE
Dariusz Strąpoć,
dstrapoc@slb.com

RECEIVED 03 June 2024
ACCEPTED 01 November 2024
PUBLISHED 19 December 2024

CITATION
Patiño C, Strąpoć D, Torres O, Mullins O, Bustos U, Bermudez O, López A, Trujillo M and Morales H (2024) First downhole sampling of a natural hydrogen reservoir in Colombia. *Front. Energy Res.* 12:1443269.
doi: 10.3389/fenrg.2024.1443269

In Colombia, natural hydrogen (H_2) was recently declared a source of unconventional renewable energy. An opportunity has been recognized to take advantage of information on the infrastructure of oil fields as a springboard for H_2 exploration in the country's sedimentary basins. Establishing similarities and identifying components of the possible H_2 systems in the different geological contexts where the presence of H_2 has been proven in Colombia's sedimentary basins allows the establishment of the probability of H_2 in the Ecopetrol oil and gas fields in Colombia. The components of H_2 systems include potential H_2 source rocks and reservoirs. Potential accumulations need to be confirmed through measurements, sampling, and well testing. The main types of H_2 well exploration carried out in this study resemble those in oil fields and include surface surveys, logging while drilling (mud gas and petrophysics), and downhole sampling. In the case of a hydrocarbon field in the Llanos Basin, a detailed seismic and geological review, supported by surface survey indications of H_2 traces, prompted further investigation while drilling wells in the basin to establish the provenance and distribution of H_2. Based on the proposed workflows, we evaluated possible strategies in the area. Given the positive evaluation of the possible elements of a theoretical H_2 strategy, a sampling plan was defined both in the well and on the surface that will reduce the uncertainty of the prospect of natural H_2 in the studied basin but may also be applied to similar geological settings worldwide. This study shows the application of such an H_2 exploration strategy, leading to the presented results from the first well and confirming the presence of an active natural H_2 system in the Llanos Basin.

KEYWORDS

natural hydrogen exploration, hydrogen downhole sampling, Colombia, hydrogen mud gas logging, natural hydrogen systems

1 Dawn of natural hydrogen exploration

Natural hydrogen (H_2) is emerging as an attractive clean energy for the future due to its minimal carbon footprint, high future economic margins compared to other forms of H_2 generation, and energetic characteristics. The generation of natural H_2 has been identified in various regions of the world and in different geological contexts. Although there is already an H_2 production field in Mali, Africa, the large-scale exploitation probabilities of H_2 in other places in the world are not yet apparent. The forefront of exploration today is in Australia (Withcombe et al., 2024), the United States, and France, where tenders and offers for exploration blocks have been opened; drilling has started in the first two. Within the areas where H_2 has been found, there are also sedimentary basins with oil production activity (Australia and, in this study, Colombia) or accidental discoveries in water wells (Mali and Kansas, USA). In recent years, dedicated drilling has begun in areas with potential natural H_2 systems. However, no significant accumulation has yet been reported.

2 Introduction to the Llanos Basin geology as a potential natural hydrogen system

2.1 Basement and hydrogen source rocks

To understand natural H_2 generation systems, it is important to establish an analogy between the basement as a possible so-called source rock and the petroleum system's kitchen since without the source there would be no H_2 production. In most cases, the basement is the rock formation in which H_2 generation occurs and from which H_2 is released. Most basement rocks associated with H_2 production have mafic/ultramafic characteristics, high iron content, and/or high concentration of radioactive elements; these rocks favor serpentinization or iron oxidation processes and/or water radiolysis. These processes require the presence of percolated waters or aquifers to interact with the basement rocks, promoting natural chemical reactions that release the H_2. The geomechanical conditions of the alteration and/or other mechanisms that favor the exposure of a rock volume to water improve the production per unit area of H_2 in the system. In the Llanos Basin, the areas of the basement with high heat flux and/or with hydraulic head-driven water influx were the key elements of the targeted natural H_2 system (Figures 1, 2). This implied the need for not only suitable source rock at adequate H_2-kitchen temperatures in the case of potential serpentinization but also continuous delivery of the substrate water needed for water radiolysis.

2.2 Hydrogen kitchen

The presence or interaction of water is essential for H_2 genesis. Water is the source of free H_2 in the Earth's crust due to its reduction by minerals or ores containing Fe^{2+}or via radiolysis by radioactive elements (see the extensive list of natural H_2-forming reactions in the subsurface by Boreham et al., 2021). Chemical reactions that occur with mafic or radioactive rocks give rise to this hydrogen release. The lower acidity and higher temperature of the water trigger or promote H_2 production since they catalyze or accelerate the water reduction reactions—serpentinization (McCollom et al., 2020). Hence, geothermal anomalies are believed to be related to favorable environments for the generation of natural H_2 at higher rates. The main characteristics of the Llanos Basin are its active and extensive aquifers, given the powerful recharge of meteoric waters in the foothills area, toward the basin's eastern limit. López-Ramos et al. (2022) suggested that in different locations of the basin, the recharge has varying contributions from different directions that result in diverse geothermal and compositional characteristics for each area. In the evaluation area, analysis of water from the basin suggests a greater deepening of the meteoric waters to the east because they arrive at a higher temperature than in the surrounding fields. This condition implies that water may have traveled from deeper areas—probably from the crystalline basement (Figures 2, 3). This favors the likely participation of these waters in serpentinization or radiolysis processes and, in turn, their help in advective aqueous media transport of theoretically generated hydrogen produced in these deep zones. Hence, the basement in this part of the basin is mostly granitic, dioritic, and phyllitic, so water radiolysis might be the main H_2-forming mechanism (but both can contribute), independent of temperature. That may imply that in iron oxidation and water radiolysis, importance may shift in magnitude across the basin depending on temperature and rock radioactivity, respectively.

2.3 Migration

Contrary to what occurs in hydrocarbon exploration, the temporal relationship that exists in this case between the H_2 migration stages, the production stages, and the associated H_2 volumes does not hold the same relevance because H_2 is assumed to be continuously replenished due to the geological cycle of crustal and mantle rocks. Therefore, unlike hydrocarbons, H_2 is not produced in restricted windows of time of adequate thermal maturity of certain organic-rich lithologies. This indicates that the H_2 being produced now originates in recent geological times and hence does not require exploration for ancient accumulations. Instead, due to its mobility, H_2 can be found in recently formed traps along main generation and leakage fairways.

Once H_2 is released, its migration to the surface or toward natural traps is easy as it is a gas with a very small molecular size that is capable of passing through most materials with minimal porosity, except for nonfractured crystalline rocks such as mafics or evaporites like thick and laterally extensive salt layers. Faulting/fracturing in crystalline basements, as in the Llanos Basin (Figure 2), could exponentially multiply the contact area of the reactive rocks with incoming water and, therefore, exponentially multiply the possibilities of the release of the generated excess of H_2. Such release could initially occur in the dissolved aqueous phase H_2 (aq) if the H_2 flux is lower than that required to saturate the water's flow rate, which could be the case for the Llanos Basin.

2.4 Possible reservoirs and seals

Due to the small molecular size of H_2, practically any type of rock with minimal porosity and permeability can store it. It should be noted that analogous to self-sourced unconventional petroleum reservoirs, rocks that tend to have active H_2 recharges will represent a greater target for exploration since H_2 concentration in them is expected to be higher. Dynamic aquifers with active surface seepage can also be active H_2 storage locations and constitute the main interest when evaluating reservoirs. Hence, dissolved H_2 carrier beds may lead to gas cap/phase accumulations up-dip or under conditions of oversaturation. The molecular size of H_2 is 0.24 nm, and the

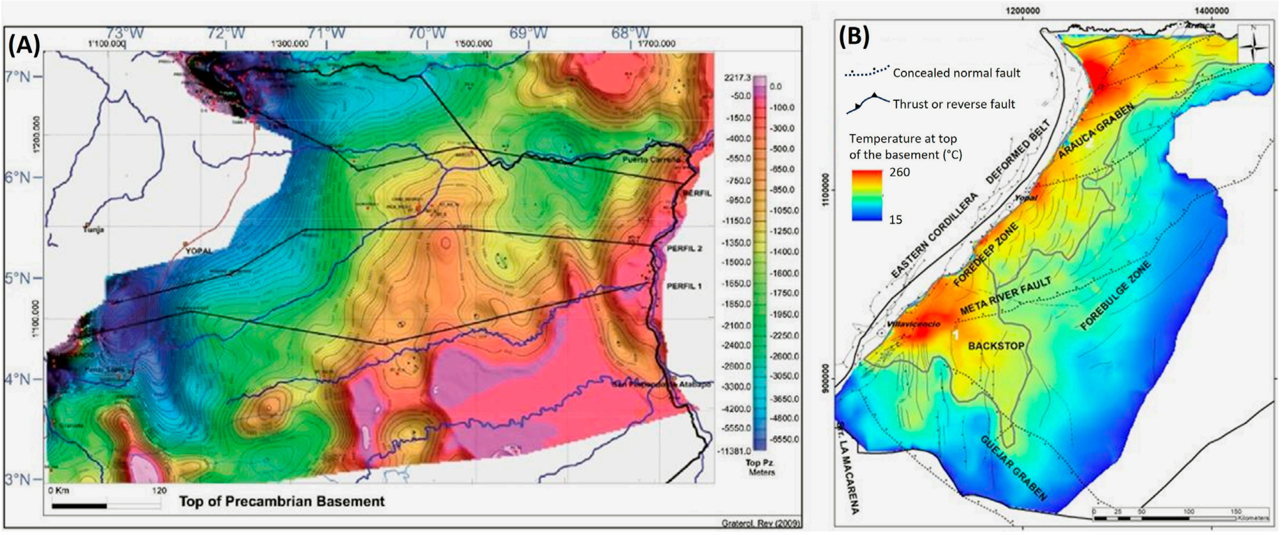

FIGURE 1
Llanos Basin maps of interest for the definition of natural H_2 generation potential associated with the Precambrian and crystalline basement: **(A)** top of the Precambrian basement; **(B)** relative heat flux at the crystalline basement (López-Ramos et al., 2022) within the outline of the basin and with the main fault populations highlighted.

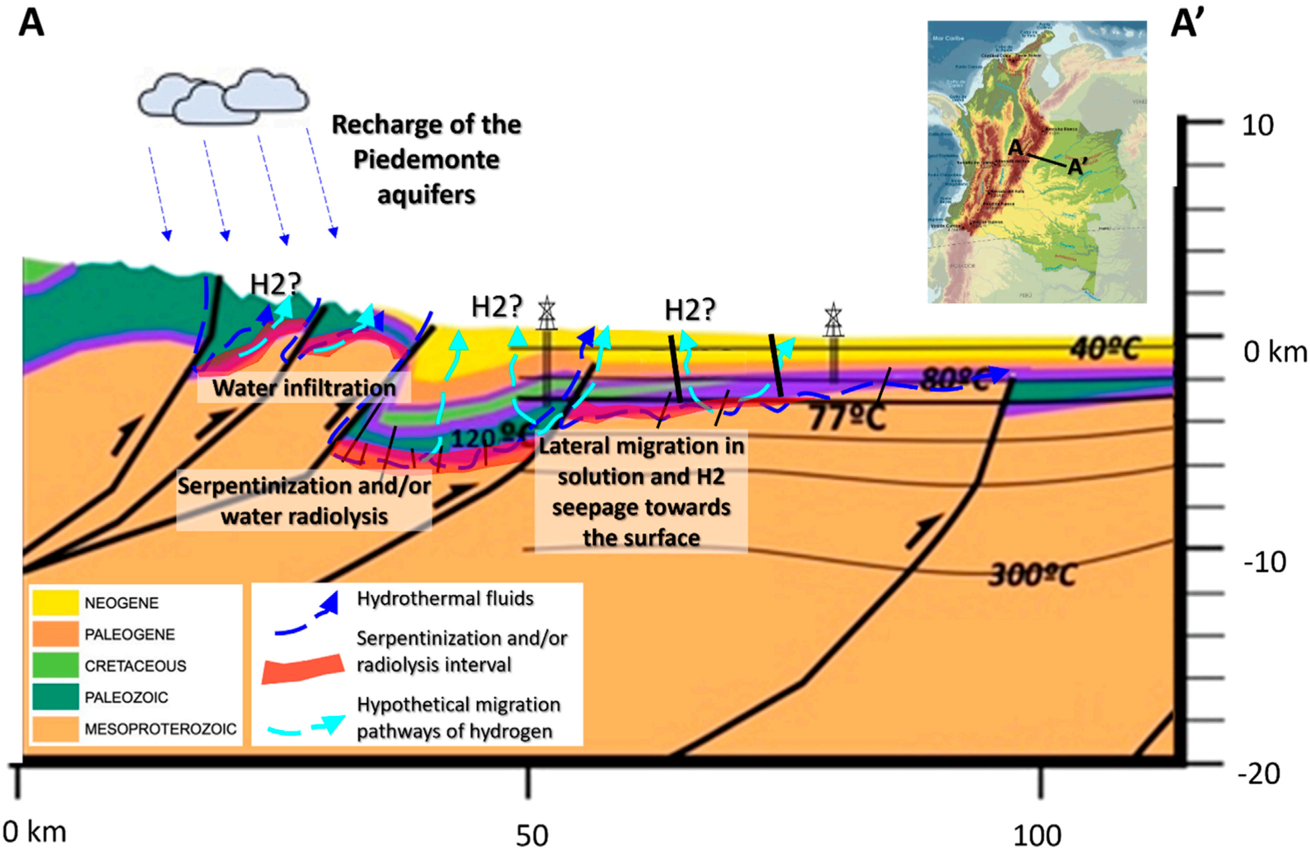

FIGURE 2
Schematic section of Colombia’s Llanos Orientales Basin **(A, A')**, modified by López-Ramos et al. (2022). Intervals in purple highlight potentially active H_2 generation zones within the upper sections of the basement reacting with conceptualized water influx. The most promising are the fault blocks, where the ultramaphics basement is at temperatures that guarantee a fast rate of serpentinization.

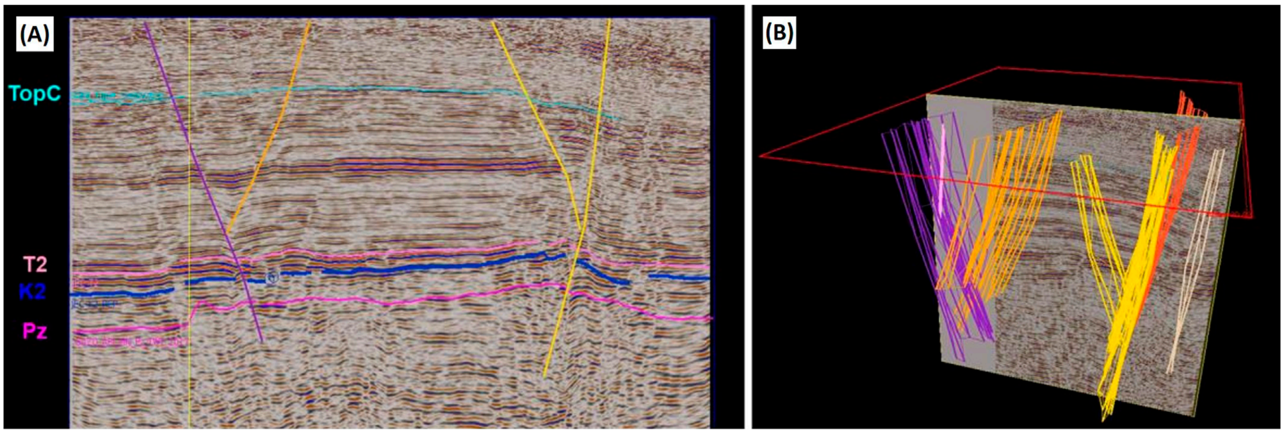

FIGURE 3
(A, B) Interpretation of 3D seismic data showing the main faults, which are noticeable features from the crystalline basement to the surface. The exact position of this seismic line in the basin cannot be revealed (Patiño et al., 2023a).

rocks that act as seals in petroleum systems have microporosities with apertures of nearly 2 nm, so only transitional gas trapping of dissolved H_2 can occur. In Mali, the seal rock has been characterized as dolerite—a crystalline rock without intrinsic porosity and whose texture, without secondary fracture-permeability, does not allow hydrogen to leak (Maiga et al., 2023). Another type of rock capable of effectively trapping H_2 is salt in the evaporitic sequences, and green H_2 storage is being proposed and evaluated in voluminous post-mining salt caverns (Ozarslan, 2013).

The main challenge when defining a hydrogen "play" concept in any basin in Colombia is the type of seal and its capacity to effectively trap H_2 in the aqueous or gas phase. In this study, the possibility of a type of play associated with the main faults that would conduct H_2 from the crystalline basement to the surface is proposed. However, in the Llanos Basin, the crossing of the basin-wide León shale formation (Figure 4), characterized by very low permeability, would create a funnel effect that would reduce or delay the continuous migration of H_2 and could form sectors with a major H_2 accumulation under the shale and near the interpreted faults.

3 Surface-based hydrogen exploration

3.1 Basin-scale seismic

The interpretation of deep faults in the existing seismic data has great relevance for understanding the possible migration paths for H_2 from the crystalline basement to the surface via advection and diffusion effects. The presence of these faults may help explain the migration of H_2 to the surface. The main faults would be responsible for crossing the entire sedimentary sequence, from Paleozoic through to Mesozoic and Cenozoic to the present in the area, and for distributing H_2 in the permeable layers or even bringing it to the surface (Figure 3). In the area (onshore), no surface morphologies associated with surface H_2 seepages like those described in the literature, such as "fairy circles," were identified. However, the lack of these structures is not a definitive indicator of the lack of a hydrogen kitchen in the basin (Truche et al., 2024) —for example, due to microbial consumption in the crust's biosphere, especially in the soil. Since these morphologies do not exist, the projections of the main faults that originate in the basement to the surface are identified as the most prospective areas for surface surveying, sampling, and verifying the presence of H_2 in this part of the basin. Figure 4 shows the proposed concept of the funnel effect overlain on the interpreted seismic image of the field, showing regional seal shale also supported by the petrophysical response of the Mesozoic and Cenozoic formations.

3.2 Seepage surveys

From a remote sensing perspective, surface geomorphic anomalies have special significance in the exploration of hydrocarbons (Gupta, 2017) and H_2. In the case of the "Carolina bays" (Zgonnik et al., 2015) or "fairy circles" (Myagkiy et al., 2020), these depressions are considered the surface expression of H_2 emanations from the underground to the surface. These geomorphological features favor the initial approach of explorers to an area and drive the concentration of technical and economic resources. Many authors (Halbouty, 1976; Saunders et al., 1999; Schumacher, 1996; Almeida-Filho et al., 2010; Gupta, 2017) have noted obvious examples of geomorphic anomalies related to hydrocarbon leaks, establishing a precedent among the surface effects that can be created by the emanation of gases to the surface. Geomorphic anomalies generally appear as circular to oblong and elongated features, which are distinguishable from the environment in terms of features such as topography, image tone, vegetation, soil, soil moisture, and surface roughness, with often hazy boundaries (Gupta, 2017). All these features are recognizable via remote sensing.

Geomorphic anomalies are identified mainly from the interpretation of drainage patterns and their disturbances (Ibanez et al., 2007) in the Llanos Basin. Generally, anomalous expressions correspond to radial or annular drainage

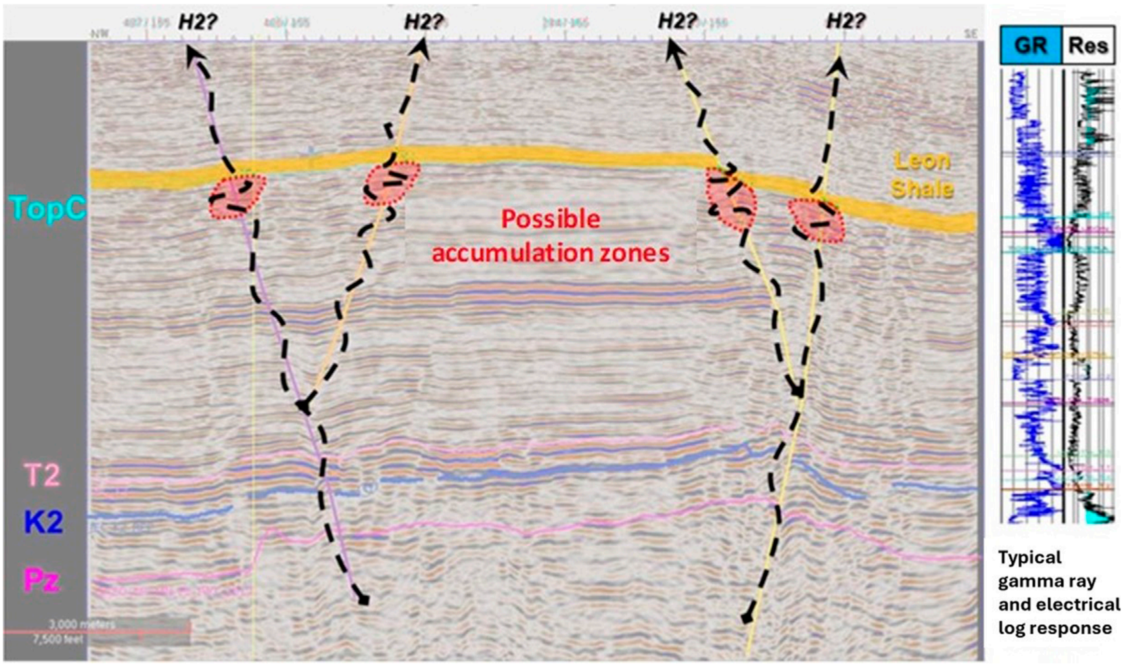

FIGURE 4
Seismic cross-section of Llanos Basin: a theoretical concept of a gas trapping via funnel effect, which could facilitate the accumulation of H_2 (Patiño et al., 2023a). Orange highlight: regional seal, with the Leon shale below it, which is the hypothesized transient H_2 trapping mechanism.

patterns that show dome-like geomorphic features or depressions. These features can correspond to anticlines, domes of different natures, and alteration chimneys due to gas microleaks. In the case of depressed expressions, these are generally identified by the formation of circular or elongated bodies of water. They may correspond to faults, which represent potential conduits of gases from depth to surface.

In practical terms, the identification of geoforms must be accompanied by an initial characterization of the mineralogy—the presence of alteration minerals. These can be identified with spectral mapping techniques in optical images, and the characteristics of vegetation, such as the state of plant health, senescence, and species abundance or absence, are identifiable in optical images using spectral band algebra. The geomorphic anomaly presented in Figure 5 was identified using the automated interpretation of the drainage from the 12.5 m PALSAR DEM (radiometric terrain correction) and applying the "sun shading" technique (Cooper, 2003), using optical imaging, ASTER, and SENTINEL 2.

3.3 Surface gas sampling

The surface sampling stage of exploration seeks to acquire surface data of H_2 in the soil. This should follow the stages involving remote sensors and indirect methods, like seismic interpretation, since this information is collected to define the best locations to capture gases at shallow depths that indicate migration from the underground to the surface. The procedure was similar to the capture of discrete soil-gas sampling. However, the considerations of detecting and capturing the smallest molecule include special materials and established sampling protocols that seek to ensure that a sample is taken in the shortest possible time to avoid any losses. In addition, there must be a blank sampling procedure to reduce uncertainties and artifacts inherent to the sampling process. Accordingly, we developed a procedure based on the premises described above to preserve gas samples until their laboratory analysis. During sampling, a gas measurement was carried out in the field, which was used as backup data to compare with the laboratory results. In the soil samples taken in the Llanos Basin, H_2 concentrations were 100–1,132 ppm (Patiño et al., 2023b). Subsequently, gas speciation and concentration measurements performed in a specialized laboratory resulted in comparable data.

4 Subsurface hydrogen hybrid exploration with petroleum

This section demonstrates how different petroleum system tools and techniques have been adapted for natural H_2 exploration, including mud gas logging, petrophysical logging, and downhole sampling. This adaptation includes the well that initially targeted shallow petroleum deposits and was extended deeper to search for H_2 accumulations and source rocks.

4.1 Mud gas logging techniques

4.1.1 Analyzer calibration

The main objective of this research was to characterize the H_2 metrology using the DQ1000™ Mass Spectrometer Gas Analyzer.

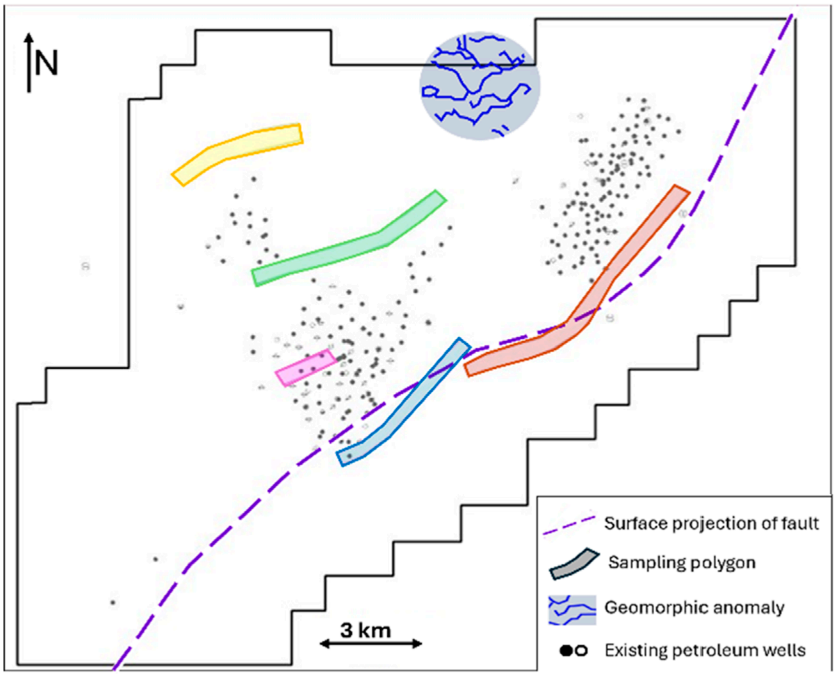

FIGURE 5
Surface sampling areas of H_2 seepage based on seismic interpretation. Sampling areas shown around the surface expression of an example major fault and a nearby geoform. Source: Ecopetrol S.A.

The tool is used globally as a mud gas analyzer in exploration for hydrocarbons that use air as a carrier gas. It is also used for logging while drilling selected inorganic gases. This characterization was required to obtain quantitative H_2 logging and provide realistic concentrations of this new energy resource, for which exploration and assessment have intensified recently. The calibration of this mass spectrometer was not a straightforward process for several reasons. First, the reading at the mass over charge ratio equals 2 (m/z = 2), corresponding to the molecular ion of H_2, which is impacted by background noise. This background noise, called the "m/z = 1 blast effect," varies between machines and can drift over time. Another challenge is that the H_2 signal is strongly exaggerated or amplified by this analyzer. Additionally, the pattern of the H_2 amplification is complex. Detailed testing of multiple mass spectrometers using multiple gas mixtures followed by in-depth data analysis provides a better understanding of the pattern. Ultimately, the improved quantification of the H_2 method of the DQ1000 Mass Spectrometer was developed and recommended for deployment prior to logging any well in which H_2 might be the main or auxiliary target (Strąpoć et al., 2023). The method involves several H_2 mixtures at different concentrations, which allows the contraction of a linear signal transformation. This method also provides minimum and maximum (saturation) levels of the quantitative range of an individual DQ1000 system based on its background H_2 reading and its m/z = 2 signal exaggeration established by the calibration procedure. A typical mass spectrometer is characterized by the quantitativeness of H_2, ranging from 50 ppm to approximately 15–20% by volume.

4.1.2 Drill bit metamorphism H_2 generation

Drill-bit metamorphism (DBM) is a drilling process where the drill bit, rock, and drilling fluid react at high temperatures, cracking and breaking down artificial gases (hydrocarbons and non-hydrocarbons) in mud, which return to the surface (Wenger et al., 2009). The most common DBM-related gases are ethene, propene, and butene (unsaturated hydrocarbons) and, gaseous alkanes and CO_2, CO, COS, and H_2 (Faber et al., 1988). In H_2 exploration, a distinction of natural H_2 from DBM-added H_2 is of key importance and can be flagged with other DBM-specific gas species such as ethene. Such non-DBM H_2 concentrations corrected for analytical bias can then be normalized per rock volume using flow rates (mud and air in flow pumps and degassing chamber), borehole volumetrics, and rate of penetration (ROP). This normalized quantitative H_2 provides realistic H_2 concentration in drilled formations. However, there is a risk of overprinting drill-bit metamorphism-derived H_2, which could be corrected for in oil-based mud (OBM) drilling if logging of ethene, propene, or CO is deployed (Strąpoć et al., 2020; Strąpoć and Fornasier et al., 2022). This methodology aids emerging natural H_2 exploration with a quantitative mud gas logging tool. C_2H_4 (ethene) is one of the main alkene molecules used to distinguish DBM-related gases. Direct mass spectrometers, used while drilling to read surface mud gas, can obtain close to pure ethane in mass over charge m/z ion 30 and a mix of ethane + ethene ion m/z 26. Part of this study methodology is to obtain C_2H_4 from these spectrometers. First, these two masses need to be cleaned of recycling, background, and baseline gases. Then, based on the fragmentation in the mass spectrometer by the ion

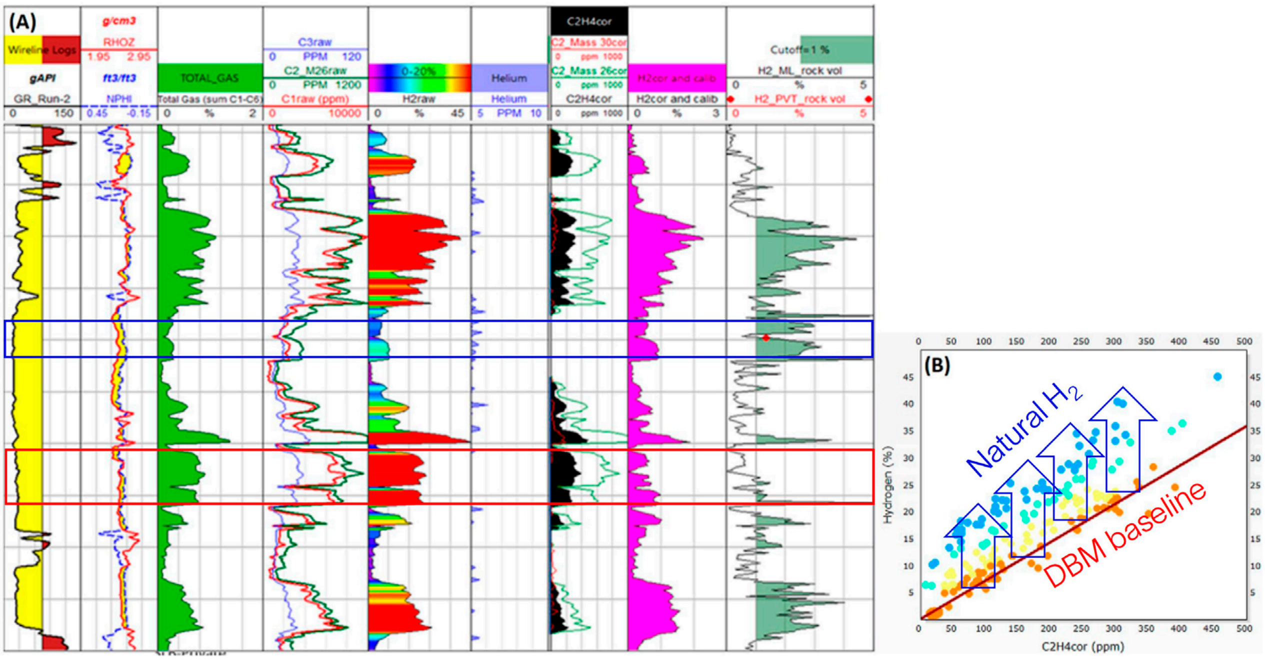

FIGURE 6
(A) Geochemical mud gas log from an exploration well in Llanos Basin showing raw gas readings (C1–C3 alkanes, H_2, and helium), ethene calculation proxy, calibrated H_2 signal corrected for drill-bit metamorphism in vol% of the mud gas carrier by air to the analyzer, and, finally (far right) H_2 normalized per rock volume drilled in volume at ambient conditions (includes the red data point for downhole sample normalization as described in the text). **(B)** Crossplot showing co-generation of H_2 and ethene (C_2H_4) by DBM from OBM, where any data point above the DBM baseline (orange) contains contribution of natural H_2: proxy used to correct the raw signal for DBM overprint.

source, the basic subtraction of these two masses must be divided by 2.28 (according to the NIST Standard Reference Database) as follows:

$$C_2H_4cor = (26cor - 30cor)/2.28,$$

where *cor* means cleaning by recycling or baseline gases on mass 26 and from recycling and shoulder effect (from nitrogen molecule, mass 28) on mass 30. In this study, C_2H_4cor will be the variable used to filter out artificial hydrogen, as shown in the crossplot graphic of Figure 6.

4.1.3 Hydrogen normalization per drilled rock volume

Once mud gas data are corrected for all drilling-related artifacts, the following technique leads to the quantification of gas species per mud volume and, subsequently, per drilled rock volume. The liberation of formation gas due to drill-bit milling of the rock allows the assumption of a representative amount of gas entrained in a volume of mud circulating per unit of time at the bottom of the drilled well. Such a correction is an industry standard and includes the mud flow rate recorded by the flow pumps, wellbore diameter, and the ROP of the drill bit. The resulting gas concentration data, corrected by the mud flow rate at the degasser *versus* its air flow rate, allows for the derivation of moles per volume of mud and, ultimately, moles and volume at surface conditions per volume of drilled rock (Figure 6).

Translating the moles of H_2 to volume at surface conditions (1 bar, 25 °C) provides a one-dimensional estimate of H_2 resources along the trajectory of the well. It is assumed that all gas is released from the rock by the crushing action of the drill bit and that all gas is entrained in the mud volume that has swept past the drill bit. Additionally, as shown by Strąpoć and Fornasier et al. (2022), gas remains firmly entrained in the mud until reaching the degassing device (mud degasser). Degassing efficiency depends on the type of drilling fluid and the thermal and physical treatment of the mud flowing through. Specifically, the mud flow rate, agitation rate, heating temperature (if any), and finally the flow rate of the headspace gas phase—here, air—are responsible for stripping away the released mud gas. A gas extraction efficiency study (Strąpoć and Fornasier et al., 2022) has shown that the behavior of H_2 and methane in oil-based mud (OBM, used in this well) is very similar in terms of the extraction rate. The efficient release of H_2 from mud in the degasser device permits a limited error of underestimation of its entrainment in mud concentration. Certainly, the cumulative propagated error H_2 concentration in surface volume per volume of drilled rock is large, yet it provides a realistic resource estimate continuously along the exploratory wells.

Another challenge of such low intrinsic permeability reservoirs, where the gas primarily occupies the joints, fractures, or faults, is that mud gas data can appear as sudden spikes. What remains unknown is the level of spreading of small-scale feature gas spikes within the upward-traveling mud volume *versus* the cycle time of the surface mud gas analyzer. Therefore, caution is needed in interpreting the mud gas data, especially when normalizing it over the entire reservoir section. Figure 6 shows that in many sections of the drilled interval, the observed mud gas H_2 concentration correlates with that of ethene (C_2H_4) generated by the drill-bit metamorphism of the oil-based mud. Only certain sections of the reservoir show less DBM levels, yet still highlight significant H_2 target zones for H_2 downhole sampling. Ultimately, the final reservoir H_2 concentration was compared with petrophysical logs; their integration dictated the decision on the wireline downhole fluid sampling strategy.

4.2 Petrophysical logging

Petrophysical analysis rests on three foundations: density neutron, advanced spectroscopy, and nuclear magnetic resonance. Advanced spectroscopy is a pulsed neutron wireline-conveyed tool that can be logged both in open- and cased-hole conditions. The device has a pulsed neutron generator (PNG) and one detector. The gamma ray energy spectra acquired during predefined time gates in the tool detector are processed to provide a complete set of elemental yields. The relative yields are then converted to absolute dry-weight concentrations via the oxide closure model (Grau and Schweitzer, 1989; Herron et al., 2011). The difference between the total measured carbon and total inorganic carbon (TIC, fraction of the total carbon contained within minerals in the rock matrix) provides the formation's total organic carbon (TOC) (Pemper et al., 2009). The TOC here was very important for confirming that the reservoirs were water-bearing sands. In addition, the dry frame matrix density, matrix neutron, matrix photoelectric factor, and matrix sigma are also obtained from the elemental dry weights. The matrix information is critical to achieving matrix-corrected porosity outputs for both density and neutron, thus leaving any potential porosity deficit due to formation fluid effects. The mineral volumes were obtained by a machine-learning approach based on variational autoencoder frameworks (Craddock et al., 2021). This technique relies on the quantification of common mineral concentrations in sedimentary formations using input measurements of atomic element concentrations from spectroscopy logs. An algorithm involves inputs, encoders, outputs, and cost functions for coefficient optimization during the training process. The inputs are the dry-weight concentrations of atomic elements (and their associated uncertainties), with outputs of the dry-weight fractions of 14 minerals. Inspecting the lack of porosity deficit between matrix-corrected density porosity and neutron porosity outputs, respectively, labeled as DPHI_MC and TNPH_MC in Figure 7, in addition to zero TOC values across the cleaner reservoir sections, confirms that the reservoirs are water bearing. In this study, we incorporated continuous nuclear magnetic resonance (NMR) transverse relaxation (*TH2*) measurement from an eccentered pad-type device. The purpose was to obtain pore size distribution (rock quality assessment), matrix-independent porosity (for assessing potential porosity deficits vs. nuclear logs due to hydrocarbon presence), irreducible water saturation estimation (to derive continuous free-water saturation), and continuous permeability estimates to support the determination of the optimum zones for acquiring dynamic tester information and formation fluid samples. Due to oil-based mud as the drilling fluid, we found that 52 milliseconds was an optimal *TH2* cutoff to split between free vs. bound fluid fractions on the NMR *TH2* signal.

The main sandstone lobes contain free fluid volumes of approximately 10 p.u. and permeabilities close to 100 mD. The NMR permeability was compared and adjusted against mobility points from dynamic testers. The good correlation between mobility points and continuous NMR permeability using the Timur–Coates equation suggests that reservoir mobility is mostly driven by pore-size distributions. In addition, a good correlation between NMR pore size distribution and clay volume from spectroscopy was observed. The combination of spectroscopy, magnetic resonance, and matrix-corrected porosity supports the dynamic tester pressure acquisition program. Once the pressure points were taken and mobility vs. NMR permeability was adjusted, the formation fluid sampling points were defined. Regarding the comparison of natural H_2 from mudlogging data and electrical logs, we observed some correlation between "high natural H_2" zones and larger T_2 distributions in the NMR signal. The next step to be treated in a technical study would be nuclear and NMR modeling to attempt detection and quantification of natural H_2, thus achieving continuous hydrogen-related petrophysical outputs.

4.3 Downhole sampling

Openhole wireline formation sampling is widely used around the world for both formation oil and formation water sampling. There is always concern about obtaining a clean formation sample with minimal or no contamination from invaded mud filtrate in the drilling fluid. Openhole wireline formation tools and methods have been developed to minimize this contamination. In all cases, longer pumping times for wireline sample acquisition are used to reduce contamination levels of mud filtrate in the recovered sample. For immiscible sampling, such as formation water sampling in wells drilled with OBM, the contamination is a separate phase, so removal of the bulk of contamination is trivial. However, in the case of sampling formation H_2, there is possible contamination of H_2 from DBM. Initially, any H_2 DBM will be in the OBM; this filtrate can then enter the formation in the normal filtrate invasion process. The question then arises as to whether measurable H_2 from DBM could transfer from the oil to the water phase during the time from initial filtrate invasion during and after formation sample acquisition, finally terminating at the point of physical separation of the oil and water phases of the acquired sample. Convective mixing of the water and oil in the formation is limited mainly to the relatively short periods of bulk mass transfer during filtrate invasion and sample acquisition. Diffusive mixing is relatively slow. It is highly unlikely that all DBM-H_2 would have the time to dissipate by any mechanism into the nearby formation water.

H_2 solubility greatly depends on pressure and temperature. Nevertheless, (nonpolar) H_2 is much more soluble in aliphatic solvents than in water, so if there is any mass transport of H_2 from one phase to the other, the transfer of natural H_2 from formation water to OBM filtrate contamination is more likely from a solubility standpoint than the transfer of DBM-H_2 from OBM filtrate to formation water. As noted above, H_2 migration from one phase to the other in the formation is not fast. In any event, to test for any possible DBM-H_2 contamination originating in the OBM filtrate and leaching into the formation water sample, multiple formation water samples were taken at the same sampling depth station at different times. These samples varied significantly in the quantity of the filtrate. Ultimately, samples with very low contamination were

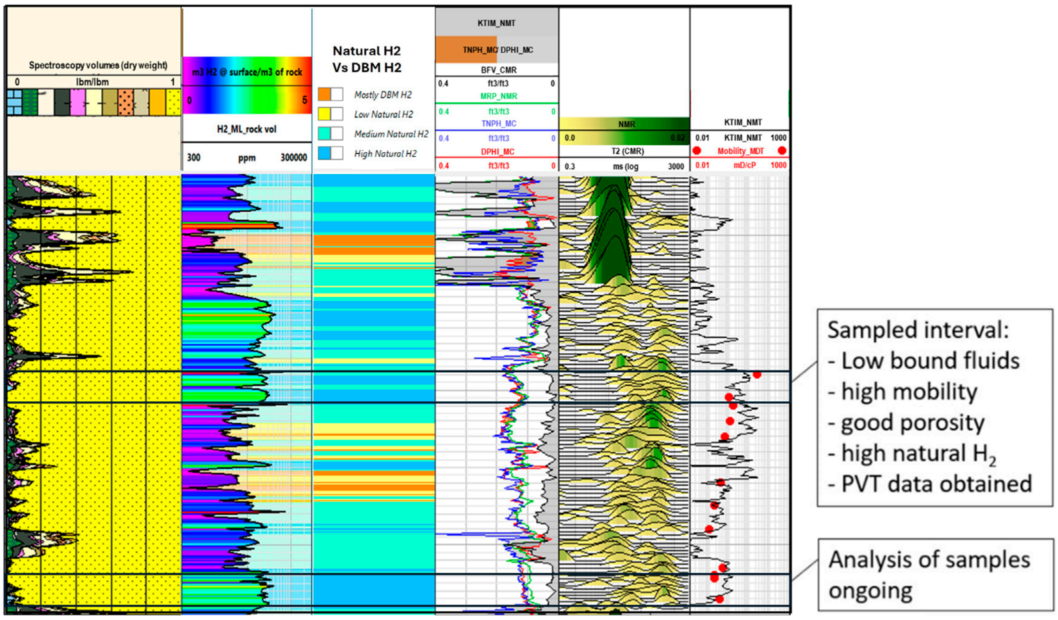

Sampled interval:
- Low bound fluids
- high mobility
- good porosity
- high natural H_2
- PVT data obtained

Analysis of samples ongoing

FIGURE 7
Integration of interpreted petrophysics (elemental spectroscopy to mineralogy content; NMR TH2 spectral distribution and mobility) and mud gas geochemistry (calibrated raw H_2 readings, corrected for DBM and normalized per rock volume in volume at ambient conditions), logs driving wireline modular drill stem tester (MDT) measurements and sampling points (rightmost track).

obtained. Samples with more filtrate would be expected to have more DBM-H_2 if (and only if) this is a significant contaminant. The fact that the quantity of H_2 detected in the formation water had no dependence on the fraction of contamination indicates there is no significant DBM-H_2 in these samples. It should be noted that all H_2 was collected from the sample bottle liquids, whether water or oil.

Based on petrophysics-based proxy logs (mobility and water saturation) and indications from H_2 richness from mud gas and the magnitude of DBM-H2 in the reservoir section, a dedicated downhole sampling strategy was designed. The outlined high-water saturation and mobility interval were ranked based on natural H_2 richness. Overlapping best-chance intervals for successful sampling were targeted. Due to the relatively low solubility of H_2 in water, standard pressure-compensated sampling was used to prevent gas phase separation and direct contact of H_2 gas with the steel body of the bottles. In addition to reservoir fluid sampling, the wireline tool sampled the mud filtrate. After surface transfer of the pressurized fluid above reservoir pressure, flash phase separation was performed in a PVT laboratory. The contamination level with the OBM filtrate of each reservoir fluid sample was estimated. The exsolved gas phase and residual liquid phase were analyzed for H_2 concentration. The reservoir samples were corrected for H_2 content found in the filtrate fraction. Using petrophysics-derived porosity (~11%) and quantified H_2 amount per reservoir water volume at reservoir conditions, we derived the richness of dissolved H_2 in volume at surface conditions per rock volume of the reservoir (~1.1 vol./vol.) and mass (~0.9 g/m3). The result of this downhole sample was comparable to the normalized mud gas H_2 from the equivalent depth (~1.3 vol./vol., rightmost log track in Figure 6). However, in the sampling depth vicinity, the normalized H_2 log shows significant variability. This methodology needs to be confirmed with more comparisons of downhole samples.

5 Learnings from the first downhole hydrogen samples in the context of the natural hydrogen system

The proposed methodologies and workflows in this study mainly consider the reviews in terms of updated technological monitoring and surveillance carried out worldwide, along with constant communication with experts who are references throughout the world, about the search and identification of natural H_2 genesis/accumulations. The main objective was to carry out a preliminary review of the theoretical elements of a probable H_2 system in the eastern Llanos Basin of Colombia. In addition, this methodology is proposed as a guide for a first review and use of existing data in an oil field that can be useful for defining H_2 presence. Dedicated exploration was deployed on the field and basin scales. Initial surface surveys of H_2 in soil were based on seismic prospecting of the Llanos Basin. This basin is also under oil and gas exploration drilling, and in areas of overlapping petroleum and H_2 potential, we used a mud gas logging technique (described above) that monitors hydrocarbons (C1–C10) and inorganic gases, including H_2 and helium. The evaluation of a significant H_2 resource after it is identified must include the H_2 origin, establishing the existence of the kitchen and its type. There are similarities between the geological configurations of some of the basins where natural H_2 has been detected worldwide and the possible generation systems at the Llanos Basin. The circular surface geoforms were H_2 seepage areas, yet without detectable impacts on the soil mineralogical or floral assemblages. In terms of lithology, in this case, there are no known mafic or ultramafic rocks in the basement, no volcanic influence, and no associated helium or NH_2 detected. Instead, granites, diorites, and phyllite are the basement at a depth of 13–15 km. The level of radioactivity, natural fracture density, and ferric iron content remain to be investigated. However, there are advantageous elements of the Llanos Basin system that increase natural H_2 potential: the presence of hydrothermal activity and foothill aquifer recharge imply high hydraulic head and likely deep penetration of water via deeply seated faults in the system with a high geothermal gradient. Additionally, the granitic basement can contribute to H_2 generation via water radiolysis, and the sedimentary system contains promising seals.

Consequently, the nature of the reservoir in the area explored so far has proven to be water-saturated with dissolved gases—perhaps a dissolved-H_2 carrier bed. Despite low H_2 solubility in water at surface conditions, it is enhanced at elevated pressure and temperature—for example, 0.077 weight % (0.386 mol/kg of pure water) at 150 °C at 400 bar (4 km depth of hydrostatic pressure), 8.65 vol./vol., or 8.65 L of H_2 at surface conditions per 1 L of water at reservoir conditions (Zhu et al., 2022). Due to the literature-based study on H_2 solubility at these downhole conditions, we were confident that we could safely deploy the standard pressure-compensated wireline downhole sampling system. By keeping the H_2 in solution and avoiding phase separation, we minimized the risk of damage to the steel-based components of the tools. The gas in solution allowed for the use of the normal practices of sampling such fluids, which require premeditated calculations of phase behavior using measured *in situ* fluid (wireline) pressures and concentrations, such as those from calibrated, corrected for artifacts, and normalized mud gas readings. These H_2-calculated estimates must be juxtaposed against maximum H_2 solubility in the formation water. In this study, we used the worst-case scenario of pure water with the highest H_2 solubility, but we recommend including downhole salinity evaluation to not overestimate H_2 solubility for safety reasons. Ultimately, these concentrations per rock volume serve as a guideline for targeted downhole sampling and testing of promising intervals, specifically in hypothetical up-dip or sub-seal gas phase accumulations, pending an efficient trap or adjacent to large gas conduits such as large faults (the funnel concept—Figure 4). Although the relatively high concentration of H_2 observed in the drilled rock was confirmed by downhole sampling at reservoir pressure, no estimations of flow rate, reservoir pressure, or accumulation size are guaranteed. Further testing of the pressure support of the reservoir and the sustained production rate is necessary to properly evaluate the reserves.

6 The way forward

The current study serves as an example of a basin-scale proof of concept for natural H_2 system exploration, starting with basin modeling, field simulation, and deep regional seismic and geohydrological studies, leading to surface surveys and ultimately drilling with advanced hydrogen logging and downhole reservoir fluid sampling. This workflow has proven that the concept of the "play" is correct; the system has i) H_2-generation mechanisms, potentially renewable, via natural hydrothermal water circulation, ii) migration conduits via faults and dynamic aquifers, and iii) likely transient trapping mechanism under a basin-wide shale formation. Further research should evaluate potential trap structures associated with this shale and the connection to the kitchen via deep faults that likely deliver H_2. Preferentially, gas phase accumulations can be found where the water-dissolved H_2 has reached concentrations beyond the bubble point, either due to cumulative H_2 influx or to water depressurization as it migrates upward (via faults or up-dip in the carrier beds). Successfully identified H_2-containing intervals, even if in oil and gas wells, should be isolated and flow-tested to allow for a technoeconomic assessment of this decarbonized energy resource. Therefore, this study contributes to establishing a standard approach for natural H_2 exploration across the energy industry.

Data availability statement

The datasets presented in this article are not readily available because this study is based on data already published by Ecopetrol (see citations) or proprietary Ecopetrol's data released for this study, which include data obtained from commercial services provided to Ecopetrol by SLB. Requests to access the datasets should be directed to Cesar Augusto Patiño Suarez.

Author contributions

CP: conceptualization, formal analysis, funding acquisition, methodology, visualization, and writing–original draft. DS: conceptualization, formal analysis, funding acquisition, methodology, visualization, writing–original draft, and writing–review and editing. OT: data curation, methodology, and writing–original draft. OM: methodology and writing–original draft. UB: methodology, visualization, and writing–original draft. OB: formal analysis, investigation, and writing–review and editing. AL: formal analysis, investigation, and writing–review and editing. MT: formal analysis, investigation, and writing–review and editing. HM: formal analysis, investigation, and writing–review and editing.

Funding

The author(s) declare that financial support was received for the research, authorship, and/or publication of this article. Financial support was received for the research and authorship from Ecopetrol Upstream and Low Emissions Vice Presidency. SLB has sponsored the publication fee and time spent by the SLB co-authors on this research and creating the manuscript.

Acknowledgments

The authors thank the Ecopetrol S.A. Upstream Vice Presidency (Exploration/Development), Low Emissions Vice Presidency, Innovation Vice Presidency, and HOCOL S.A. (Ecopetrol Group) for granting permission to publish these data and for their support of this study. They also thank the Instituto Colombiano del

Petroleo (ICP) and service companies, including EXPRO, for their participation in the analyses during this project.

Conflict of interest

Authors CP, OB, AL, MT, and HM were employed by Ecopetrol. Author DS was employed by SLB, France. Author OT was employed by SLB, Colombia. Authors OM and UB were employed by SLB, United States.

The authors declare that this study received funding from Ecopetrol Upstream and Low Emissions Vice Presidency. The authors declare that this study received funding from SLB. Both funders had the following involvement in the study: study design, collection, analysis, interpretation of data, the writing of this article, and the decision to submit it for publication.

The author(s) declared that they were an editorial board member of Frontiers, at the time of submission. This had no impact on the peer review process and the final decision.

Publisher's note

References

Almeida-Filho, R., Ibanez, D. M., and de Miranda, F. P. (2010). Interpretação morfoestrutural com dados SRTM no auxilio a exploração petrolifera: um exemplo na bacia sedimentar do Amazonas. *Rev. Bras. Geofis.* 28, 89–98. doi:10.1590/S0102-261X2010000100007

Boreham, C. J., Edwards, D. S., Czado, K., Rollet, N., Wang, L., Van der Wielen, S., et al. (2021). Hydrogen in Australian natural gas: occurrences, sources and resources. *APPEA J.* 61, 163–191. doi:10.1071/AJ20044

Cooper, G. R. J. (2003). Feature detection using sun shading. *Comput. Geosci.* 29, 941–948. doi:10.1016/S0098-3004(03)00091-8

Craddock, P., Srivastava, P., Datir, H., Rose, D., Zhou, T., Mosse, L., et al. (2021). "Enhanced mineral quantification and uncertainty analysis from downhole spectroscopy logs using variational autoencoders," in *Petrophy.* 62 (6): 614–629. doi:10.30632/SPWLA-2021-0069

Faber, E., Gerling, P., and Dumke, I. (1988). Gaseous hydrocarbons of unknown origin found while drilling. *Org. Geochem.* 13, 875–879. doi:10.1016/0146-6380(88)90240-9

Grau, J., and Schweitzer, J. S. (1989). Elemental concentrations from thermal neutron capture gamma-ray spectra in geological formations. *Nucl. Geophys.* 3, 1–9.

Gupta, R. P. (2017). "Remote sensing geology," in *Remote sensing geology*. Third edition (Springer Nature). doi:10.1007/978-3-662-55876-8

Halbouty, M. T. (1976). Application of Landsat imagery to petroleum and mineral exploration. *AAPG Bull.* 60, 745–793. doi:10.1306/c1ea35b4-16c9-11d7-8645000102c1865d

Herron, M. M., Grau, J., Herron, S. L., Kleinberg, R. L., Machlus, M., Reeder, S. L., et al. (2011). "Total organic carbon and formation evaluation with wireline logs in the Green River oil shale," in *SPE-147184, presented at the SPE annual technical conference and exhibition*. Denver, USA: SPE. 30 October–2 November.

Ibanez, D. M., Almeida-Filho, R., and Miranda, F. P.De. (2007). Uso de dados SRTM no auxílio à pesquisa de hidrocarbonetos na Bacia Sedimentar do Amazonas. *An. XIII Simpósio Bras. Sensoriamento Remoto*. 21–26.

López-Ramos, E., Gonzalez-Penagos, F., A. Patiño, C., and López, A. (2022). Low - medium enthalpy geothermal resource assessment in deep reservoirs of the Llanos Basin - Colombia. *Cienc. Tecn. Fut.* 12, 13–44.

Maiga, O., Deville, E., Laval, J., Prinzhofer, A., and Diallo, A. B. (2023). Characterization of the spontaneously recharging natural hydrogen reservoirs of Bourakebougou in Mali. *Sci. Rep.* 13, 11876. doi:10.1038/s41598-023-38977-y

McCollom, T. M., Klein, F., Solheid, P., and Moskowitz, B. (2020). The effect of pH on rates of reaction and hydrogen generation during serpentinization. *Phil. Trans. R. Soc. A* 378, 20180428. doi:10.1098/rsta.2018.0428

Myagkiy, A., Moretti, I., and Brunet, F. (2020). Space and time distribution of subsurface H2 concentration in so-called "fairy circles": insight from a conceptual 2-D transport model. *BSGF - Earth Sci. Bull.* 191, 13. article nr 13. doi:10.1051/bsgf/2020010

Ozarslan, A. (2013). Large-scale hydrogen energy storage in salt caverns. *Int. J. Hydrogen Energy* 37, 14265–14277. doi:10.1016/j.ijhydene.2012.07.111

Patiño, C., Bermudez, O., López, A., Morales, H., and Marin, M. (2023a). "Methodology to identify key elements that are part of possible theoretical Natural Hydrogen generation systems for a hydrocarbon field in Colombia's Llanos Orientales," in *XX Congreso Colombiano de Petróleo, Gas y Energía organizado por Associacion Colombiana de Ingenieros de Petroleos (ACIPET)*. Cartagena, Colombia.

Patiño, C., Truillo, M., Morales, H., Piedrahita, D., Andrade, A., Colorado, E., et al. (2023b). First ever downhole sampling of a natural H2 reservoir in Colombia. *H- Nat. Summit.* 12.

Pemper, R., Han, X., Mendez, F., Jacobi, D., LeCompte, B., Bratovich, M., et al. (2009) "The direct measurement of carbon in wells containing oil and natural gas using a pulsed neutron mineralogy tool," in *SPE 124234, SPE annual technical conference and exhibition*. New Orleans, Louisiana: SPE. October 30-November 2.

Saunders, D. F., Burson, K. R., and Thompson, C. K. (1999). Model for hydrocarbon microseepage and related near-surface alterations. *AAPG Bull.* 83, 170–185. doi:10.1306/00aa9a34-1730-11d7-8645000102c1865d

Schumacher, D. (1996). "Hydrocarbon-induced alteration of soils and sediments,". *Hydrocarbon migration and its near surface expression*. Editors D. Schumacher, and M. A. Abrams (AAPG: AAPG Memoir), 66, 71–89. doi:10.1306/m66606c6

Strąpoć, D., Abolins, N., Ammar, M., and Gligorijevic, A. (2023). Mud logging of natural hydrogen. *World Pat. Appl. WO 2023/192219 A1*.

Strąpoć, D., and Fornasier, I. (2022). "Key role of regearing mud gas logging for natural hydrogen exploration," in *Full conference paper presented at SPWLA 63rd annual symposium*, Stavanger, Norway.

Strąpoć, D., Jacquet, B., Torres, O., Khan, R. M. S., Inan Villegas, E., Albrecht, H., et al. (2020). Deep biogenic methane and drilling-associated gas artifacts: influence on gas-based characterization of petroleum fluids. *AAPG Bull.* 104, 887–912. doi:10.1306/08301918011

Truche, L., Donze, F.-V., Goskolli, E., Muceku, B., Loisy, C., Monnin, C., et al. (2024). A deep reservoir for hydrogen drives intense degassing in the Bulqizë ophiolite. *Science* 383, 618–621. doi:10.1126/science.adk9099

Wenger, L. M., Pottorf, R. J., Macleod, G., Otten, G., Dreyfus, S., Justwan, H. K., et al. (2009). "Drill bit metamorphism: recognition and impact on show evaluation. SPE-125218-MS," in *SPE annual technical conference and exhibition*. New Orleans, Louisiana: SPE.

Withcombe, J., McDonald, N., Cressey, R., Hadi Subrata, B., Falloon, S., Carr, N., et al. (2024). Ramsay 1 and Ramsay 2, learnings from the first natural hydrogen exploration wells in Australia. *Aust. Energy Prod. J.* 64, 5453–5458. doi:10.1071/ep23119

Zgonnik, V., Beaumont, V., Deville, E., Larin, N., Pillot, D., and Farrell, K. M. (2015). Evidence for natural molecular hydrogen seepage associated with Carolina bays (surficial, ovoid depressions on the Atlantic Coastal Plain, Province of the USA). *Prog. Earth Planet. Sci.* 2, 31. article nr 31. doi:10.1186/s40645-015-0062-5

Zhu, Z., Cao, Y., Zheng, Z., and Chen, D. (2022). An accurate model for estimating H2 solubility in pure water and aqueous NaCl solutions. *Energies* 15 (article nr 5021), 5021. doi:10.3390/en15145021Available at: https://www.mdpi.com/1996-1073/15/14/5021